ORNL-5926

ornl

OAK RIDGE NATIONAL LABORATORY

UNION CARBIDE

Carbon-14 Immobilization Via the $Ba(OH)_2 \cdot 8H_2O$ Process

G. L. Haag
J. W. Nehls, Jr.
G. C. Young

DO NOT MICROFILM COVER

OPERATED BY
UNION CARBIDE CORPORATION
FOR THE UNITED STATES
DEPARTMENT OF ENERGY

DISCLAIMER

ORNL--5926

DE83 009881

ORNL-5926
Dist. Category UC-70

Contract No. W-7405-eng-26

CHEMICAL TECHNOLOGY DIVISION

NUCLEAR WASTE PROGRAMS
Carbon-14 Immobilization
(Activity AR 05 15 05 0, ONLWA05)

CARBON-14 IMMOBILIZATION VIA THE $Ba(OH)_2 \cdot 8H_2O$ PROCESS

G. L. Haag
J. W. Nehls, Jr.
G. C. Young

Date Published - March 1983

DISCLAIMER

OAK RIDGE NATIONAL LABORATORY
Oak Ridge, Tennessee 37830
operated by
UNION CARBIDE CORPORATION
for the
DEPARTMENT OF ENERGY

CONTENTS

CARBON-14 IMMOBILIZATION VIA THE $Ba(OH)_2 \cdot 8H_2O$ PROCESS

G. L. Haag
J. W. Nehls, Jr.
G. C. Young

ABSTRACT

The airborne release of ^{14}C from various nuclear facilities has been identified as a potential biohazard due to the long half-life of ^{14}C (5730 years) and the ease with which it may be assimilated into the biosphere. At ORNL, technology has been developed for the removal and immobilization of this radionuclide. Prior studies have indicated that ^{14}C will likely exist in the oxidized form as CO_2 and will contribute slightly to the bulk CO_2 concentration of the gas stream, which is airlike in nature (~330 ppmv CO_2). The technology that has been developed utilizes the CO_2–$Ba(OH)_2 \cdot 8H_2O$ gas-solid reaction with the mode of gas-solid contacting being a fixed bed. The product, $BaCO_3$, possesses excellent thermal and chemical stability, prerequisites for the long-term disposal of nuclear wastes. For optimal process operation, studies have indicated that an operating window of adequate size does exist. When operating within the window, high CO_2 removal efficiency (effluent concentrations <100 ppbv), high reactant utilization (>99%), and an acceptable pressure drop across the bed (3 kPa/m at a superficial velocity of 13 cm/s) are possible. This paper addresses three areas of experimental investigation: (1) microscale studies on 150-mg samples to provide information concerning surface properties, kinetics, and equilibrium vapor pressures; (2) macroscale studies on large fixed beds (4.2 kg of reactant) to determine the effects of humidity, temperature, and gas flow rate upon bed pressure drop and CO_2 breakthrough; and (3) design, construction, and initial operation of a pilot unit capable of continuously processing a 34-m^3/h (20-ft^3/min) air-based gas stream.

1. INTRODUCTION

The release of ^{14}C from the nuclear fuel cycle has been identified as a potential biohazard because of its long half-life (5730 years) and the ease with which it may be assimilated into the biosphere.[1-20]

In nuclear reactors, ^{14}C is produced primarily by neutron interactions with ^{13}C, ^{14}N, and ^{17}O, which are present in the fuel, the cladding, and the coolant. The bulk of the ^{14}C is released in gaseous form either at the reactor or when the spent fuel is reprocessed. Presented in Table 1 are representative release rates at various nuclear facilities.

Carbon-14, like ^{3}H, ^{85}Kr, and ^{129}I, is a global radionuclide. That is, upon release to the environment, its dosage impact is not limited to the region of release, a release which may be legislated by local government, but rather the net dosage is distributed globally in a nearly uniform manner. Furthermore, because of its long half-life, ^{14}C release poses a health hazard to both present and future generations. Modeling studies have been conducted for predicting the dosage effects from ^{14}C release. However, these studies require major assumptions concerning the effects of low-level radiation, future population growth, and time span of dosage integration. Depending upon the assumptions, total dosage estimates typically vary from 400 to 590 man-rem/Ci.

Table 1. Approximate production and release rates of several types of facilities

Facility	Rate [Ci/GW(e)yr]
Nuclear reactors	
LWR	8-10
CANDU	500
Reprocessing plants	
LMFBR	6
LWR	18
HTGR	200

Source: ref. 2.

In a modeling study by Killough and Rohwer at ORNL, a total dosage estimate of 540 man-rem/Ci was obtained. This study also predicted dosage estimates for time periods of 30 and 100 years of 18 and 23 man-rem/Ci respectively.[17] More recent modeling studies by Killough et al. have

indicated that for ^{14}C release from a 30.5-m (100-ft) stack at the Morris, Illinois, or Barnwell, South Carolina, reprocessing plants, 0.02 and 0.002% of the total dosage would occur within 100 km of the respective points of release.[18] A study by the Nuclear Energy Agency (NEA) on the release of global radionuclides ^{3}H, ^{14}C, ^{85}Kr, and ^{129}I restricted the time period of interest to 10,000 years. Hence a partial dosage for ^{14}C of 290 man-rem/Ci was used.[16] With knowledge of the worldwide release of ^{14}C, the resulting dosage per curie released, and assuming 146 fatal effects, 105 nonfatal cancers, and 76 serious genetic effects per million man-rem of dosage as estimated by Fowler and Nelson,[20] an estimate of the health effects resulting from ^{14}C release may be made. However, these health effects must be placed in proper perspective; that is, they may occur any place and any time within the time limits of dosage integration.

For global radionuclides with long half-lives, the often cited cost-effective values for controlling radionuclide release, $100 to $1000 per man-rem, may not be justified, as certain questions of a philosophical and technical nature must first be answered. However, if a technology with suitable cost-effectiveness is shown to exist, the control of ^{14}C release will then be warranted. Therefore, the primary goal of this research effort has been to develop such a cost-effective technology.

2. TECHNOLOGY DEVELOPMENT

In the development of technology for controlling the release of ^{14}C from the nuclear fuel cycle, we have established the following criteria for candidate processes:

1. acceptable process efficiency, with a nominal decontamination factor of 10,
2. acceptable final product form for long-term waste disposal,
3. excellent on-line process characteristics,
4. process operation at near-ambient conditions, and
5. acceptable process costs (<$10/man-rem).

Based upon these criteria, an operationally simple process that utilizes fixed-bed canisters of $Ba(OH)_2 \cdot 8H_2O$ has been developed at ORNL.

At ambient temperatures and pressures, this process is capable of removing CO_2 (330 ppmv) in air to concentrations <100 ppbv. Thermodynamic calculations indicate equilibrium concentrations to be at the part-per-trillion level.[21] The product, $BaCO_3$, possesses excellent thermal and chemical stability as it decomposes at 1450°C and is sparingly soluble in water, 0.124 mg-mol/L at 25°C.[22,23] Furthermore, the soluble reactant undergoes 100% conversion, thus ensuring an extremely stable material for final disposal. Gas throughputs are such that reactor size remains practical for the treatment of anticipated process streams. For a design superficial velocity of 13 cm/s, a reactor with a diameter of 0.70 m (27 in.) would be required for the treatment of a 170-m^3/h (100-ft^3/min) off-gas stream. Although extensive cost studies have not been completed, initial comparative studies with alternative technologies have indicated the process to be extremely cost competitive.[16,20,24-31] The estimated process cost is <$10/man-rem.

This report highlights the contents of two other technical reports.[32,33] For additional information, these reports should be consulted. Studies concerning the development of the $Ba(OH)_2 \cdot 8H_2O$ process for $^{14}CO_2$ removal will be broken into three areas: (1) microscale studies, (2) fixed-bed macroscale studies, and (3) design and operation of a pilot plant.

Experimental studies have concentrated upon the use of flakes of $Ba(OH)_2 \cdot 8H_2O$. As shown in Fig. 1, the material is a free-flowing solid and when reacted with CO_2 under proper conditions, the flake form remains intact upon conversion to $BaCO_3$. Vendor specifications indicate that the material is substoichiometric in water and possesses an overall hydration of 7.0 to 7.9 H_2O. Discussions with the vendor indicated that the water deficiency is intentional so as to ensure a free-flowing, nonsticking product.

The flakes are prepared by distributing a $Ba(OH)_2$ hydrate magma (~78°C) on a stainless steel conveyor belt, which is cooled on the underside with cooling water.[34] The resulting flakes have variable thicknesses [an average thickness of ~0.10 cm (1/16 in.)]. The results of a particle-size analysis on material originating from two batches are presented in Table 2. Analysis of samples obtained from these batches indicated stoichiometries of approximately 7.5 and 7.0 H_2O respectively. For a

ORNL PHOTO 6941-81A

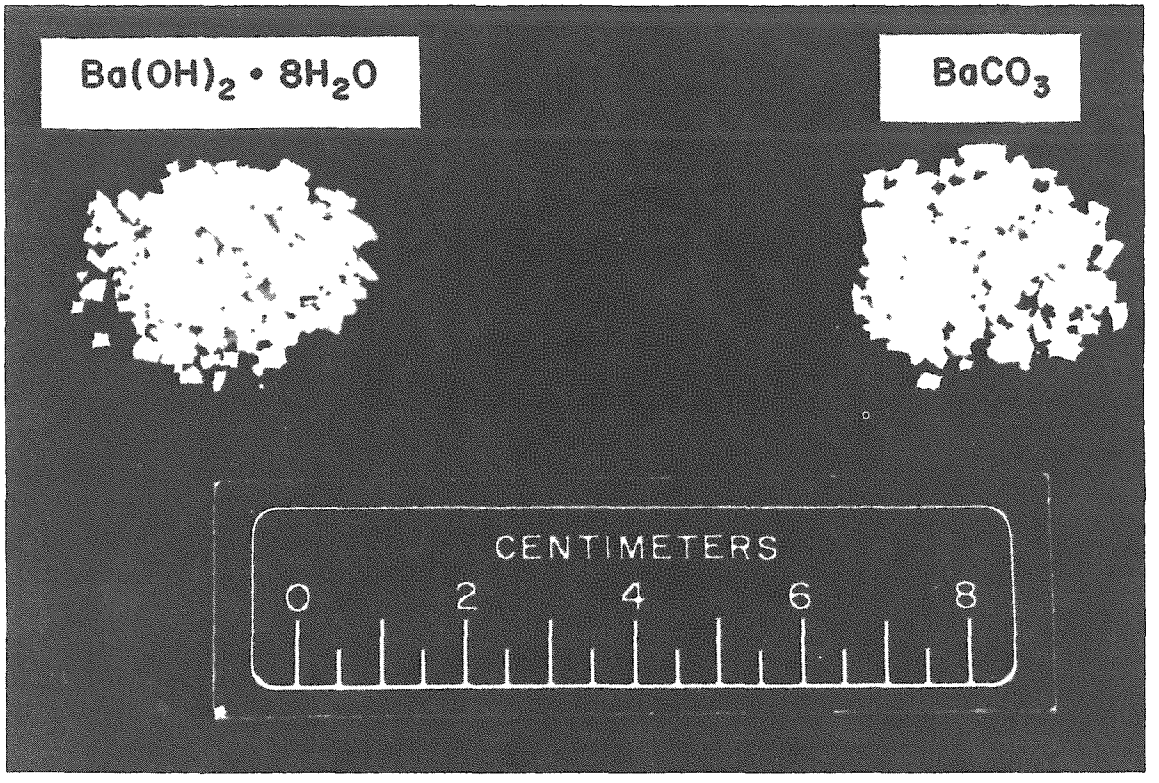

Fig. 1. Commercial $Ba(OH)_2 \cdot 8H_2O$ flaked reactant and $BaCO_3$ flaked product. The product was obtained at a process relative humidity <60%.

Table 2. Particle-size analysis of commercial $Ba(OH)_2 \cdot 8H_2O$ flakes obtained from two different batches

Particle size		Weight percent	
Mesh	mm	Batch 1	Batch 2
4 →	4.75	18.5	5.8
8 → 4	2.36 → 4.75	46.9	33.0
20 → 8	0.850 → 236	31.6	54.5
50 → 20	0.300 → 0.850	2.0	4.9
120 →	0.125 → 0.300	0.4	1.2
→ 120	→ 0.125	0.6	0.6

given batch, little variation was observed in the extent of hydration. X-ray analysis of the two samples failed to confirm the presence of $Ba(OH)_2 \cdot 3H_2O$, the next stable hydrate of lower stoichiometry. However, the existence of a $Ba(OH)_2 \cdot 3H_2O$—$Ba(OH)_2 \cdot 8H_2O$ eutectic with an overall water stoichiometry of 7.19 has been reported.[35,36] We speculated that the trihydrate species was not detected because of its small crystallite size. Sorption isotherm studies indicated that the reactant displayed negligible microporosity (mean pore diameter, $d < 2$ nm) or restrictive mesoporosity (2 nm $< d <$ 150 nm). Mercury porosimetry studies indicated that the pore size distribution was bimodal with maxima of 0.17 and 1.0 μm and that the flake porosity was 12%. When a flake was exposed to a water vapor pressure less than or greater than the vapor pressure of $Ba(OH)_2 \cdot 8H_2O$, the material either dehydrated to the trihydrate or hydrated to the octahydrate. The rates of dehydration and rehydration were determined to be functions of relative humidity. The best correlation for predicting the vapor pressure of $Ba(OH)_2 \cdot 8H_2O$ appears to be that presented by Kondakov et al.:[37]

$$\log P = -\frac{58,230}{19.155T} + 13.238 \ ,$$

where

P = pressure, Pa or nt/m^2;

T = temperature, K.

With respect to published vapor pressure data on $Ba(OH)_2 \cdot 8H_2O$, a comprehensive, chronological review of the published vapor pressures is presented in ref. 32.

As shown in Fig. 1, operating conditions exist for which the integrity of the flake form is retained upon conversion to $BaCO_3$. Because of the low molar volume of the product as compared to that of the reactant, a ratio of 0.31, and an initial particle voidage of 12%, one would predict a final product porosity of 73%. Mercury porosimetry studies have indicated product porosities of 66 to 72%.[21,32] Visual evidence of this porosity may be observed by comparing scanning electron micrographs of the reactant and product (Fig. 2).

ORNL PHOTO 1305-83

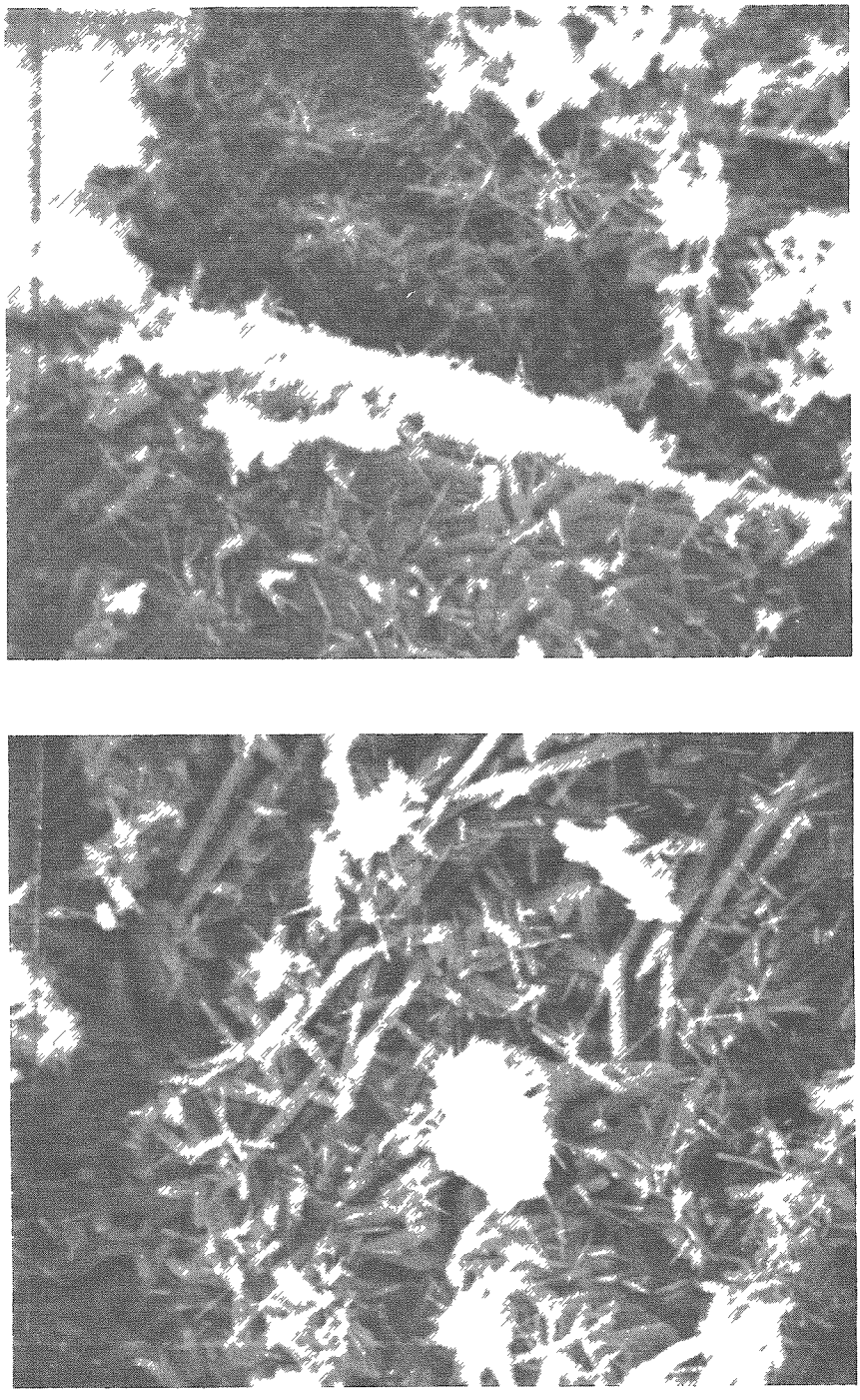

Fig. 2. Scanning electron micrographs of a flake of commercial $Ba(OH)_2 \cdot 8H_2O$ (top) and the $BaCO_3$ product. The product was obtained at a process humidity <60% (original photo, 8.9 x 11.4 cm; magnification, 5000x).

The following $Ba(OH)_2$ hydrate nomenclature will be used in the remainder of this paper: The substoichiometric flakes will be referred to as commercial $Ba(OH)_2 \cdot 8H_2O$ (7.5). Where it is of significance, the term in parenthesis will refer to the initial hydration stoichiometry. The term $Ba(OH)_2 \cdot 8H_2O$ will refer to the stable crystalline species with 8 waters of hydration.

3. MICROSCALE STUDIES

Realizing that an understanding or at least an awareness of phenomena which occur on the microscale is often required to develop an understanding of macroscale phenomena, basic studies were conducted on the hydrates of $Ba(OH)_2$ and the $BaCO_3$ product. Analytical techniques consisted of scanning electron microscopy; mercury intrusion for porosimetry determination; acid-base titrations and overall mass balances to determine the extent of conversion and hydration; x-ray diffraction analysis; single-point BET analysis; and operation of a microbalance system whereby studies of a kinetic, thermodynamic, and surface morphological nature could be performed on 150-mg samples (Fig. 3). Results from these studies were useful in characterizing the $Ba(OH)_2 \cdot 8H_2O$ reactant, which was reported in the preceding section. The intent of this section is to highlight experimental results from the microscale studies, which are as follows.

1. Methods to prepare $Ba(OH)_2 \cdot H_2O$, $Ba(OH)_2 \cdot 3H_2O$, and $Ba(OH)_2 \cdot 8H_2O$ were developed, and the presence of these species was confirmed.

2. Commercial $Ba(OH)_2 \cdot 8H_2O$ flakes were found to display negligible surface area. The rates of hydration to $Ba(OH)_2 \cdot 8H_2O$ was observed to be a function of relative humidity. For relative humidities <60%, the increase in surface area was small and the flake form remained intact. For relative humidities >60%, the flake recrystallized in a manner which resulted in greater surface area, but the increase in activity also resulted in a more fragile product.

3. Dehydration of commercial $Ba(OH)_2 \cdot 8H_2O$ to $Ba(OH)_2 \cdot 3H_2O$ and subsequent rehydration to $Ba(OH)_2 \cdot 8H_2O$ at relative humidities <60% were modeled by a shrinking core model. The relative rate was found to be dependent upon the difference between the water sorbed on the surface

ORNL PHOTO 8162-81

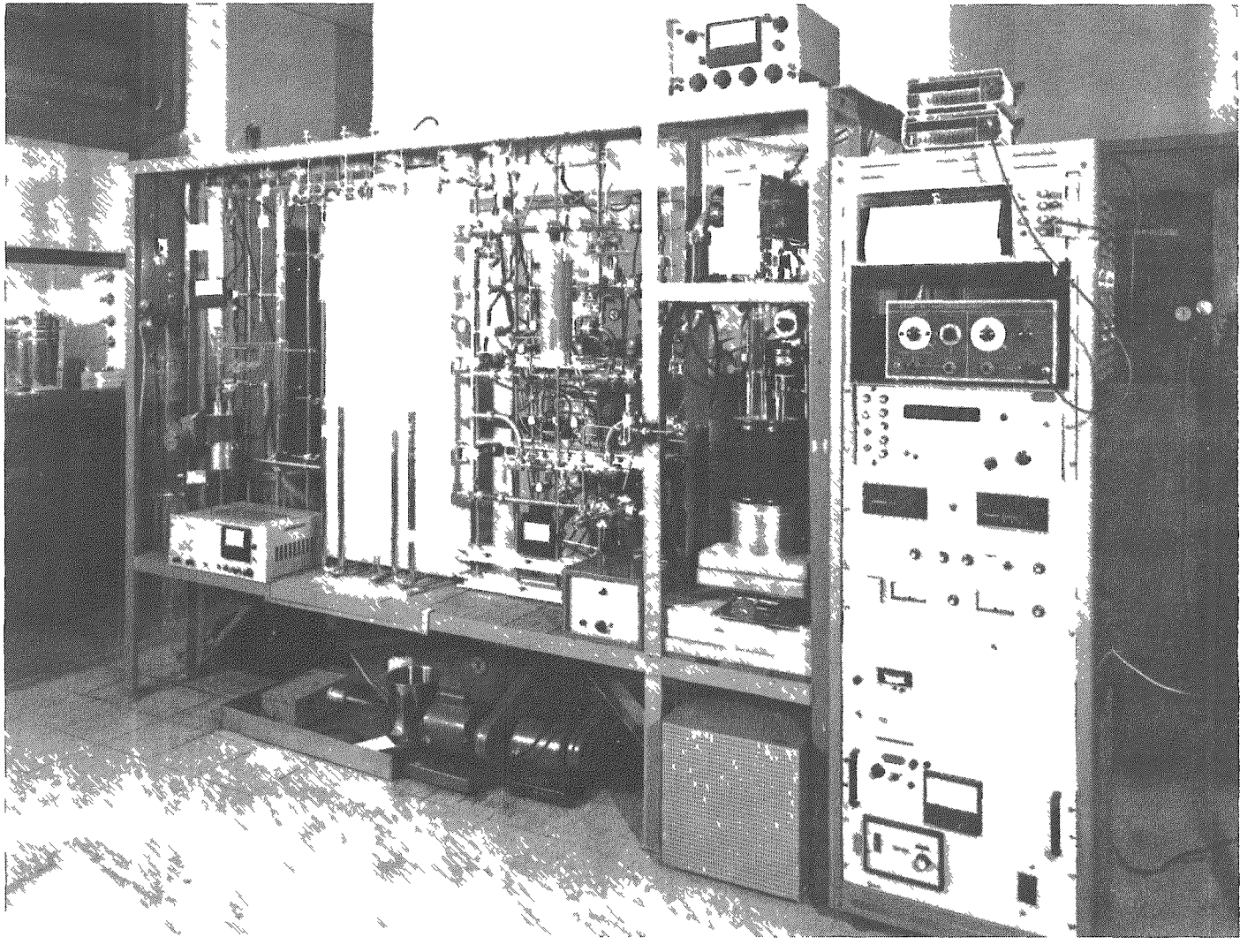

Fig. 3. The microbalance system.

for a given P/P_0 value (i.e., relative humidity) and that required on the surface for $Ba(OH)_2 \cdot 8H_2O$ to exist in a stable form.

4. There was evidence of considerable hydrogen bonding within the $Ba(OH)_2 \cdot 8H_2O$ crystal. These results paralleled the crystallography studies of Monohar and Ramaseshan in which they cited difficulty in differentiating the location of the hydroxyl ions from the waters of hydration.[38]

5. The vapor pressure correlation for $Ba(OH)_2 \cdot 8H_2O$ cited in the previous section was indirectly verified at two temperatures.

6. At low CO_2 vapor pressures, $Ba(OH)_2 \cdot 8H_2O$ was observed to be 3 orders of magnitude more reactive toward CO_2 than either $Ba(OH)_2 \cdot 3H_2O$ or $Ba(OH)_2 \cdot H_2O$.

7. For relative humidities <60%, the increase in surface area with product conversion was found to be a very strong function of the specific rate of reaction and was not a linear function of conversion.

8. The surface area of $BaCO_3$ product was determined to be a function of relative humidity. In a manner analogous to the dehydration of commercial $Ba(OH)_2 \cdot 8H_2O$ and the rehydration of $Ba(OH)_2 \cdot 3H_2O$, surface water appeared to aid in the transport of the reactant and product species, thus resulting in lower surface areas at higher values of P/P_0. However, the authors feel that the increase in surface water could not account for the drastic difference in CO_2 reactivity observed for the various hydrate species. The difference in reactivity appears to result from the additional water in the crystal structure and the greater mobility of the hydroxyl ions.

9. Based upon the analysis of nitrogen sorption isotherm data, there were no indications of hysteresis. Therefore if capillary condensation should occur, one would speculate it to result from the wall effects of noncircular pores (e.g., V-shaped points of intersurface contact).

Detailed information is available in ref. 32.

4. FIXED-BED MACROSCALE STUDIES

Over 18,000 h of experimental operating time has been completed on fixed beds of $Ba(OH)_2 \cdot 8H_2O$. These beds typically contained from 2.9 to

4.3 kg of reactant. A schematic of the experimental system, which has been described in detail in a previous paper,[21] is presented in Fig. 4. The intent of this aspect of the study was to determine the effects of air flow rate (superficial gas velocities of 7-21 cm/s), operating temperature (22-42°C), and water vapor pressure or relative humidity (0-80%) on the operational characteristics of the fixed bed, most notably the shape of the breakthrough curve and the pressure drop across the fixed bed. Since the reaction is endothermic, the reactor was jacketed and the temperatures of the influent and effluent streams were held constant. Presented in Fig. 5 is a typical breakthrough curve and pressure drop plot. For this particular run, the pressure drop increase was noticeable and was not solely a function of bed conversion.

In the course of these fixed-bed studies, it was observed that for a given mass throughput, certain process conditions resulted in a greater pressure drop than others. In several instances, the increase in pressure drop during a run behaved in an autocatalytic manner and necessitated discontinuation of the run. The increase in pressure drop appeared to result from two phenomena: a slow gradual increase that was a function of bed conversion and a rapid increase that was a function of relative humidity. The magnitude of the latter often overshadowed the former. The observed pressure drop, plotted as a function of relative humidity at two temperatures (295 and 305 K) and a superficial velocity of ~13 cm/s, is presented in Fig. 6. It is significant that the data are consistent at the two temperatures since the saturation vapor pressures differed by a factor of 1.8. Furthermore, the dependency upon relative humidity indicates the presence of a surface adsorption phenomenon. For physical adsorption on surfaces, the extent of adsorption is dependent upon the extent of saturasaturation, P/P_0, or in the case of water, the relative humidity. The fact that the pressure drop became more severe at ~60% relative humidity indicates that capillary condensation is likely present. Since no hysteresis was observed during nitrogen adsorption studies, we speculate that the condensation occurs at V-shaped contact points or pores. The presence of the condensed water then provides sites of either rapid reaction, rapid recrystallization or both. As shown in Fig. 7, flakes of commercial $Ba(OH)_2 \cdot 8H_2O$ were observed to curl during hydration when exposed to higher

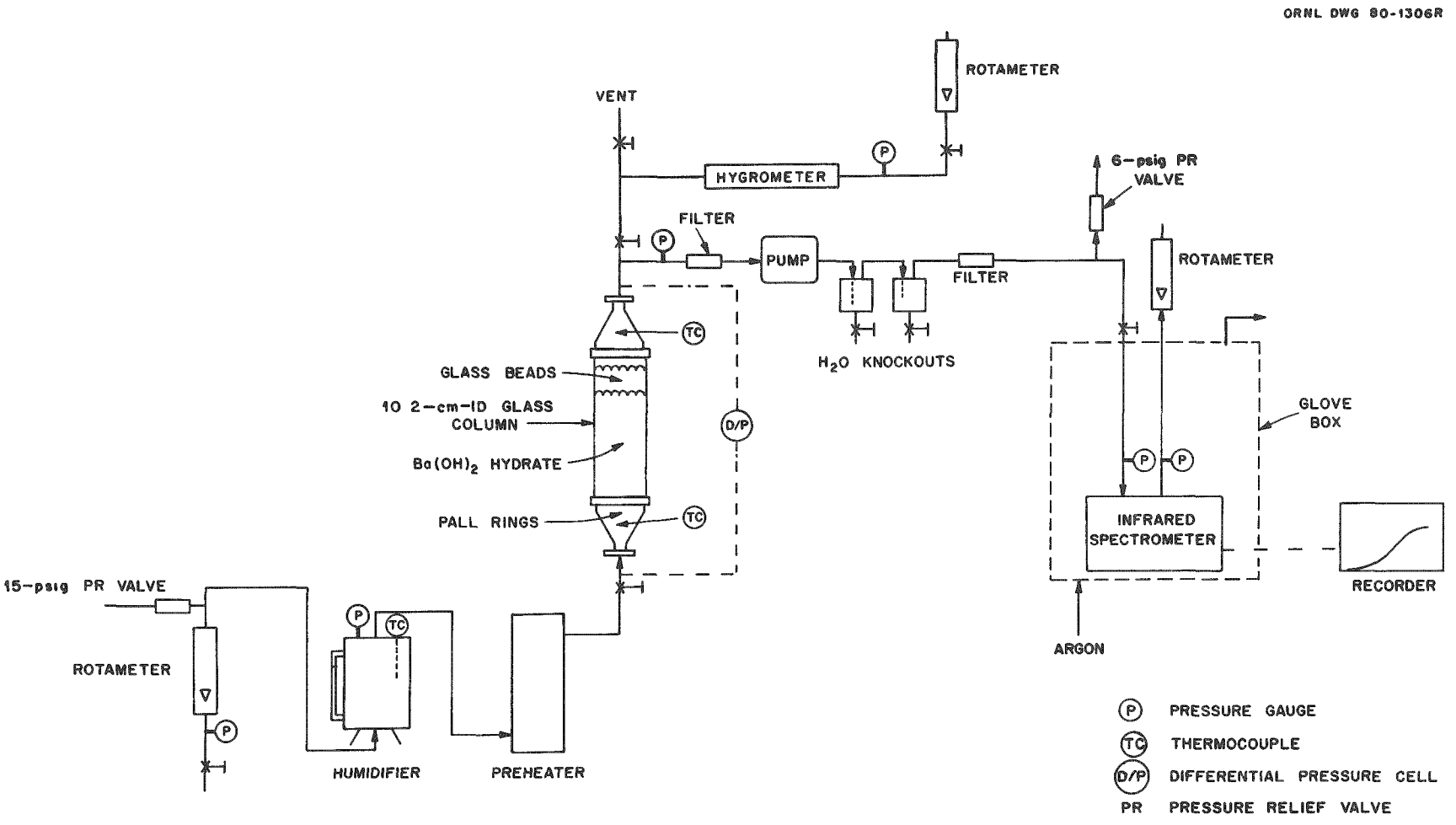

Fig. 4. The fixed-bed experimental equipment.

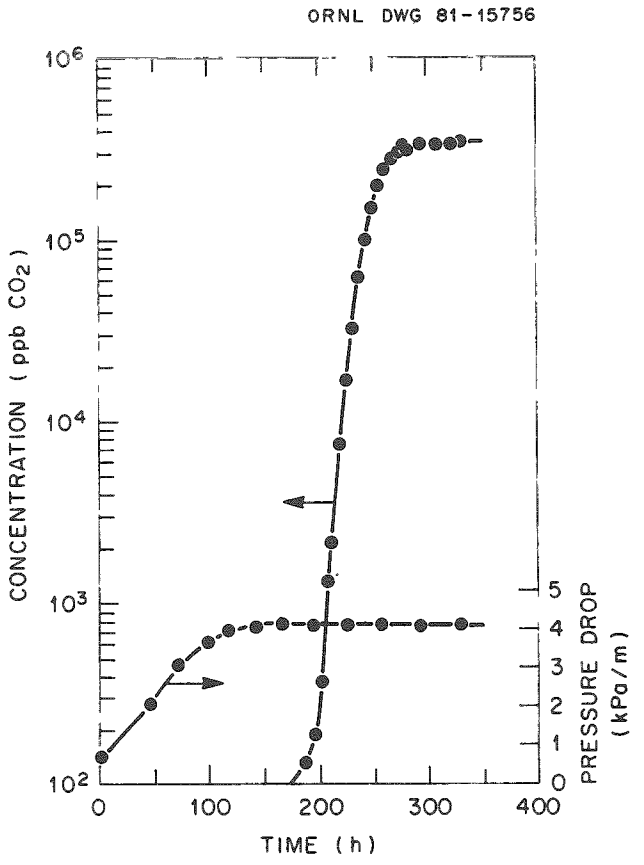

Fig. 5. Logarithm of the experimental breakthrough profile and the change in pressure drop across the bed presented as function of time (superficial gas velocity, ~13 cm/s).

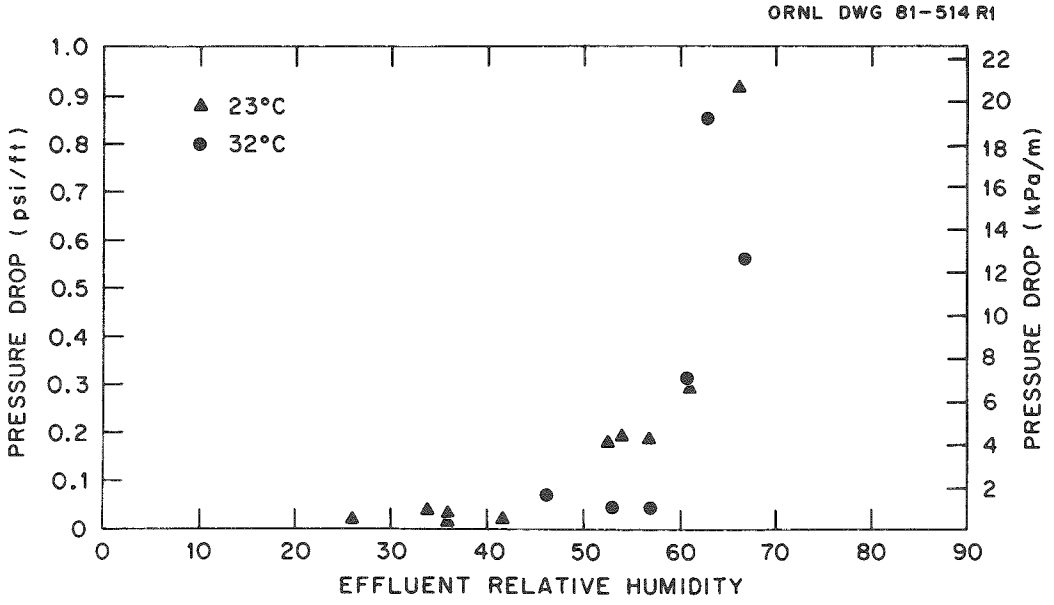

Fig. 6. Pressure drop as a function of effluent relative humidity during isothermal fixed-bed studies on commercial $Ba(OH)_2 \cdot 8H_2O$ flakes (superficial gas velocity, ~13 cm/s).

ORNL PHOTO 1306-83

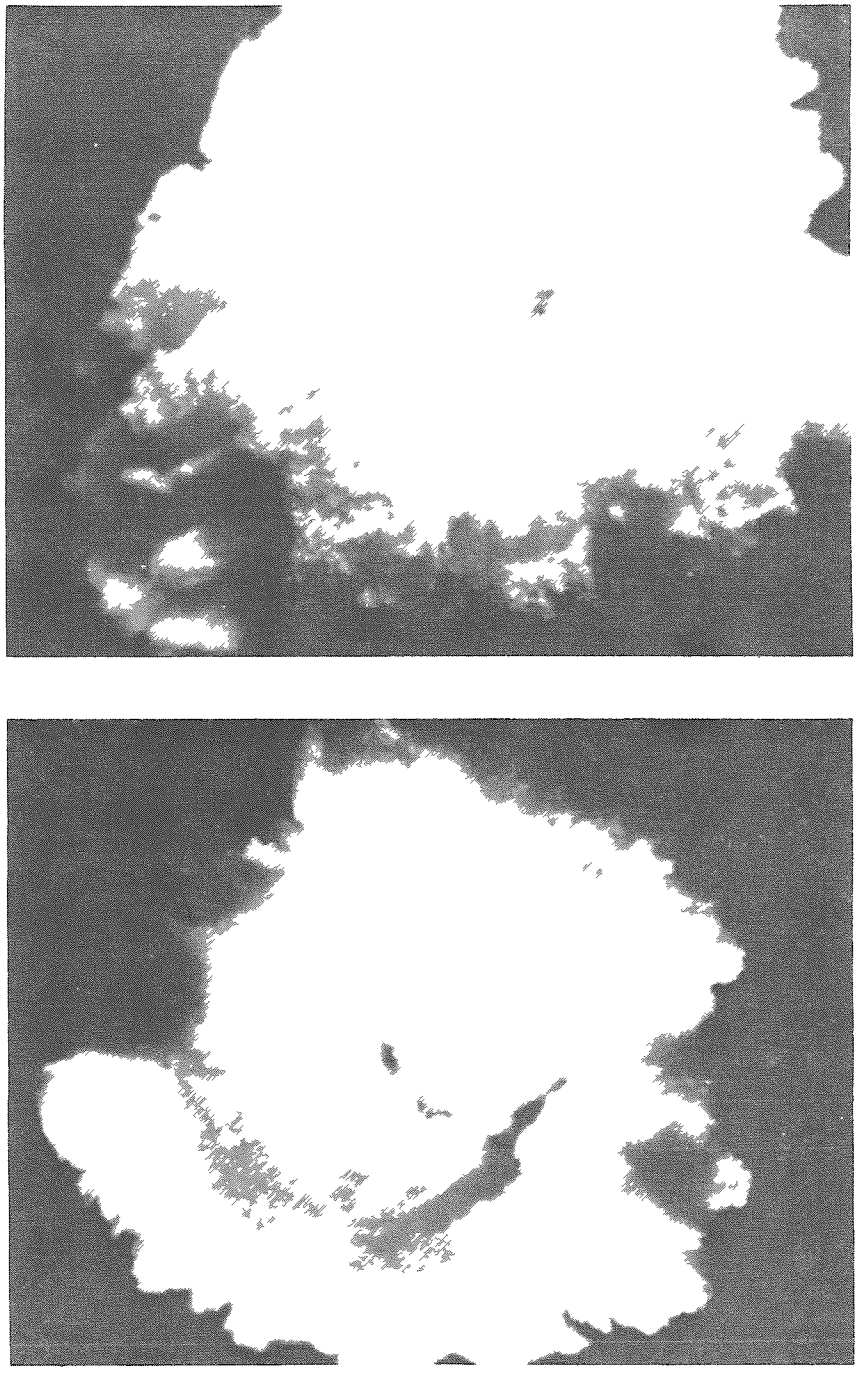

Fig. 7. Top and bottom views of a commercial $Ba(OH)_2 \cdot 8H_2O$ flake subjected to relative humidity >60%.

relative humidities. This resulted in a more fragile reactant and a carbonate product that easily degraded. Both of these factors are capable of contributing to the greater pressure drop observed at the higher relative humidities. However, experimental data from the pilot unit studies conducted under near-adiabatic conditions indicated that a second phenomenom is likely controlling. Because of the isothermal operating conditions and the relatively small contribution to the influent relative humidity from the water reaction product (6-11%) for the macroscale studies, we could not distinguish from this data whether influent or effluent relative humidity was triggering the significant increase in pressure drop. This phenomena will be addressed in more detail in the next section.

The functional dependency of pressure drop upon relative humidity is helpful in understanding the autocatalytic pressure drop behavior observed at high relative humidities. For a fixed influent water vapor concentration, any increase in system pressure at constant temperature will result in an increase in the water vapor pressure and likewise the relative humidity, P/P_0. Therefore as the pressure drop across the bed increases, so does the relative humidity within the bed, and each continues to increase until the run must be terminated. At lower relative humidities, the rate of increase in pressure drop as a function of relative humidity is not sufficient to autocatalyze the process.

The pressure drop dependency upon relative humidity also restricts the upper flow rate that the process may treat. Increased gas flows result in greater pressure drops across the bed (i.e., a greater pressure at the entrance to the bed). Therefore, the relative humidity at the entrance of the bed must be <60%, but the influent water vapor pressure must be greater than the dissociation vapor pressure of $Ba(OH)_2 \cdot 8H_2O$.

Extensive modeling studies were performed on the breakthrough curves from the fixed-bed studies. Because of the nature of the governing partial differential equations and their respective boundary conditions, solutions were of a numerical nature. An in-depth review of the method of analysis and of the associated assumptions is presented elsewhere.[32] The analysis indicated that the rate expression could be modeled by an equation of the form:

$$R = K_F A_0 (1 - X) C \ ,$$

where

K_F = gas film mass transfer coefficient,

A_0 = initial surface area available for mass transfer,

X = fractional conversion of reactant,

C = bulk CO_2 concentration.

Data analysis indicated K_FA_0 to be a weak function of temperature and a strong function of velocity, indicative of gas-film control. Considerable dispersion in the value of the K_FA_0 coefficients was observed for a given mass throughput. There were indications that the dispersion resulted from differences in the actual area available for mass transfer and the possible presence of localized channeling. Based upon published correlations for the K_F coefficient, the correlation for the K_FA_0 coefficient possessed a greater functional dependency upon velocity than expected. Because the studies were conducted on flaked material with considerable interparticle contact, we speculate that the amount of surface area available for mass transfer increased as a function of gas velocity, thus resulting in the greater than anticipated functional dependency of K_FA_0 upon velocity. This factor may also account for the greater than anticipated dispersion in K_FA_0 as some localized packing arrangements would be more conducive to restructuring. Representative breakthrough curves and the model-predicted curves are presented in Fig. 8.

5. PILOT UNIT DEVELOPMENT

In the development of this fixed-bed technology, a pilot unit capable of continuously processing an air stream of 34 m^3/h (20 ft^3/min) was designed, constructed, and is operating. Specific goals of this aspect of process development were to provide

1. the basis for the design of a ^{14}C immobilization module for future testing under hot conditions;
2. data at operating conditions not achievable with present bench-scale equipment, in particular operation at near-adiabatic conditions;
3. necessary scale-up data; and
4. operating data on key hardware items and instrumentation.

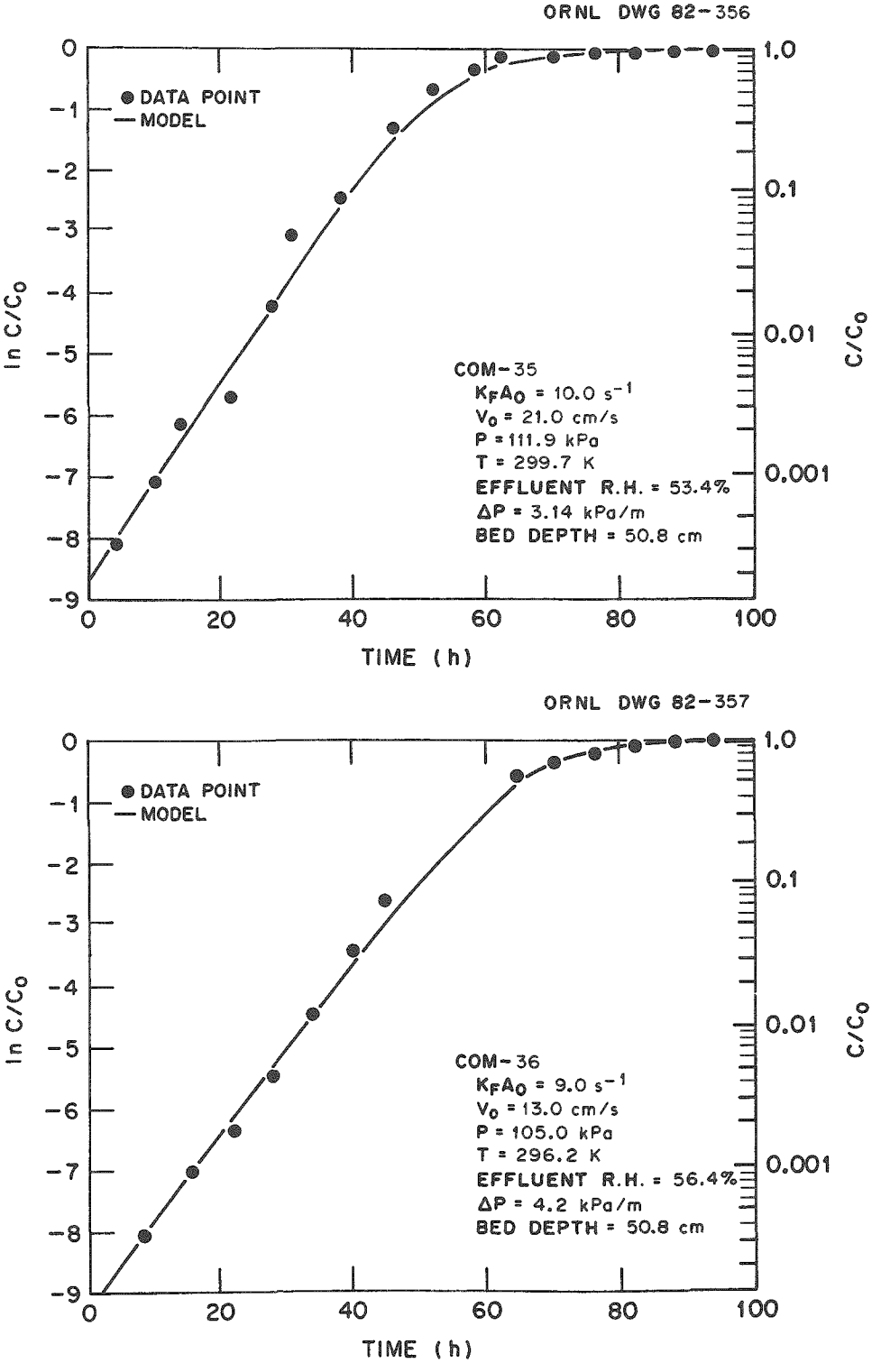

Fig. 8. Breakthrough curves and model-predicted breakthrough curves for typical fixed-bed runs.

Presented in Fig. 9 is a flow schematic of the ^{14}C immobilization pilot unit; a photograph of the system is presented in Fig. 10. The designed gas throughput at a superficial velocity of 13 cm/s in the reactor is 34 m^3/h (20 ft^3/min). The system consists of two reactors which contain canisters loaded with 32 kg (70 lb) of commercial $Ba(OH)_2 \cdot 8H_2O$ reactant. Due to the size of the canisters and the relatively long loading times prior to breakthrough, continuous operation with only two reactors is possible. The steam, air, and CO_2 flow stations are unique to our pilot unit and will not be discussed in detail.

The overall pilot unit is controlled by a 5TI logic controller manufactured by Texas Instruments. The unit is currently capable of monitoring 8 DC and 16 AC input signals and providing 24 DC and 16 AC output signals. The logic controller monitors alarm signals from the CO_2 analyzer, hygrometer, flowmeters, timers, and pressure and temperature sensors. Upon sensing an alarm condition such as a CO_2 concentration of 1 ppmv in the effluent gas stream, valves may be actuated in the proper sequence at prescribed time intervals thus diverting flow to the second column. Numerous 3/4- and 1/4-in. Whitey ball valves are located within the system for bulk flow control and for gas sampling. For valve actuation, electronic DC signals from the logic controller are converted to pneumatic signals using modular Humphrey TAC[3] electric air valves. The Whitey ball valves are then actuated pneumatically via Whitey actuators. Gas samples may be routinely taken and returned from any one of five points within the system. Sampling from these locations may be controlled by the logic controller. The sample gas is filtered and a portion of it fed to a General Eastern model 1200 APS hygrometer sensor. The unit utilizes the "vapor condensation on a mirror" principle, thus providing a true dewpoint determination. Because of the small sensor volume and the resulting small gas throughput (0.5 L/min), this portion of the gas sample is vented to the atmosphere. The remainder of the sample gas is pressurized via a metal bellows pump, fed to two knockout vessels for H_2O removal, and then moves to a Wilks-Foxboro Miran 1A infrared spectrometer. This unit, described elsewhere,[21,32] is capable of analyzing CO_2 over the continuous 100 ppbv to 330 ppmv CO_2 range. Because of the 5.6-L sensor volume and to ensure an adequate instrument response

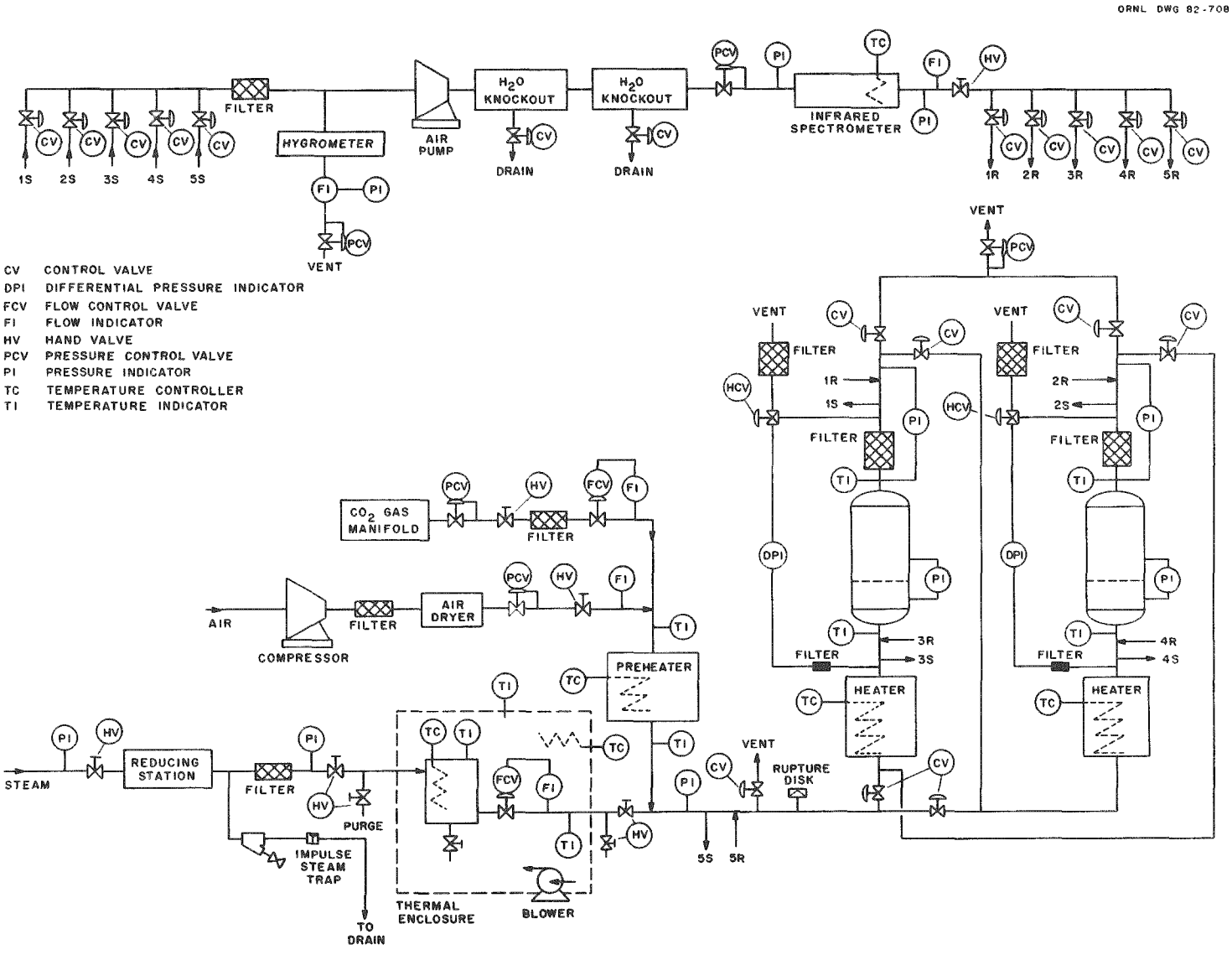

Fig. 9. The ^{14}C immobilization pilot unit.

ORNL PHOTO 2414-82

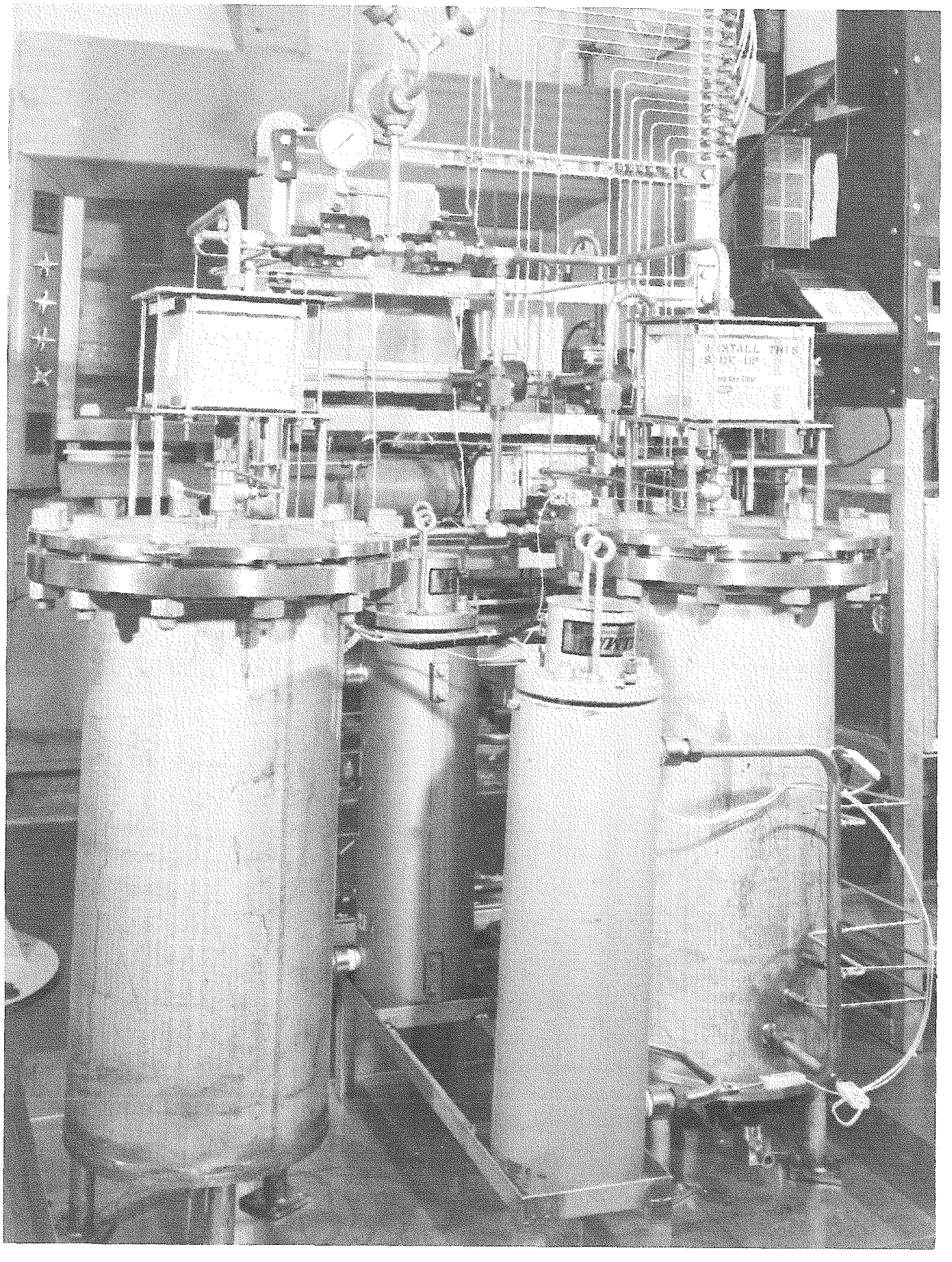

Fig. 10. The ^{14}C immobilization pilot unit.

time, the gas throughput is appreciable and the sample stream is recycled to the pilot unit.

Gas preheaters connected to Barber-Coleman series 520 temperature controllers are located before each reactor to provide the desired influent temperature. The pressure drop across each column and the gauge pressure at the base of the column are monitored via Foxboro model E13DH differential pressure cells. Dwyer Photohelix pressure gauges/switches monitor the pressure drop across the gas distributors and HEPA filters. Thermocouples are located throughout the system for temperature control and sensing.

Whereas prior studies on the 10.2-cm-ID fixed beds were conducted at near isothermal conditions and pressure drop was observed to be a strong function of relative humidity, the pilot unit studies were performed under near-adiabatic conditions (inlet gas temperature ~28°C). Under such conditions, changes in the gas stream temperature resulting from endo- or exothermic reactions are extremely important since for a given water concentration, relative humidity is a strong function of temperature. For the treatment of an air-based (330-ppmv-CO_2) gas stream, one would predict a temperature drop of ~4°C in the gas stream due to the endothermic nature of the reaction (364 kJ/mol). However, the hydration of the water-deficient $Ba(OH)_2 \cdot 8H_2O$ flakes (water stoichiometry of 7.0 to 7.9) to $Ba(OH)_2 \cdot 8H_2O$ is exothermic. A comparison of the thermal effects of the hydration and carbonation reactions indicated the hydration reaction to be relatively slow. Based upon the observed curling and recrystallization of the substoichiometric flakes and the onset of appreciable pressure drop at ~60% relative humidity (possibly attributed to capillary condensation of water vapor in pores and rapid recrystallization), we speculated that the controlling conditions were those at which the bulk of the bed hydration occurred — that is, the effluent relative humidity. It was hypothesized that flakes hydrated at relative humidities >60% were significantly more fragile and thus degraded upon conversion to $BaCO_3$.

However, consistency of the pressure drop data from the pilot unit studies performed under near-adiabatic conditions with the isothermal data discussed previously was only possible when the basis of comparison was

the influent relative humidities (Fig. 11). The addition of the water vapor reaction product and the 4°C drop in gas temperature resulted in a clear distinction between the influent and effluent relative humidities. The latter, effluent relative humidity, was roughly 30% greater. Furthermore, if the preceding hypotheses based upon effluent relative humidity were correct, one could prehydrate a bed at relative humidities <60% and then operate the CO_2 sorption process at relative humidities >>60%. Experimental studies on the pilot unit indicated that prior hydration had little, if any, effect upon the subsequent pressure drop. Therefore, based upon the conditions of the influent gas, a regime of more optimal process operation for the treatment of an air-based gas stream was defined. The influent water vapor pressure must be greater than the dissociation vapor pressure of $Ba(OH)_2 \cdot 8H_2O$ and the influent relative humidity <60% (Fig. 12). From mechanistic perspective, these observations are more difficult to explain since the portion of the unreacted bed contacting the gas stream at influent relative humidity conditions is small. Studies have indicated that the bulk of the pressure drop, when it is significant, occurs during the early stages of the run. The authors speculate that the pressure drop may result from the greater localized reaction rate at the entrance of the bed during process start-up and prior to the formation of pseudo-steady-state conversion and concentration profiles within the bed. If this should be the case, the observed pressure drop may be a one-time phenomenom and may be reduced in subsequent columns when the beds are operated in series. No such studies were conducted. However, significant degradation and caking of the beds were observed in the lower (entrance) sections. These observations are consistent with the preceding hypotheses. It is speculated that water condensing within the pores at relative humidities >60% facilitate the aqueous CO_2-$Ba(OH)_2$ reaction and aid in reactant and product transfer and recrystallization.

6. CONCLUSIONS

Extensive studies have been conducted on $Ba(OH)_2$ hydrates, their reaction with CO_2, and the operation of a fixed-bed process for CO_2 removal. Microscale studies indicated that (1) the published vapor pressure data

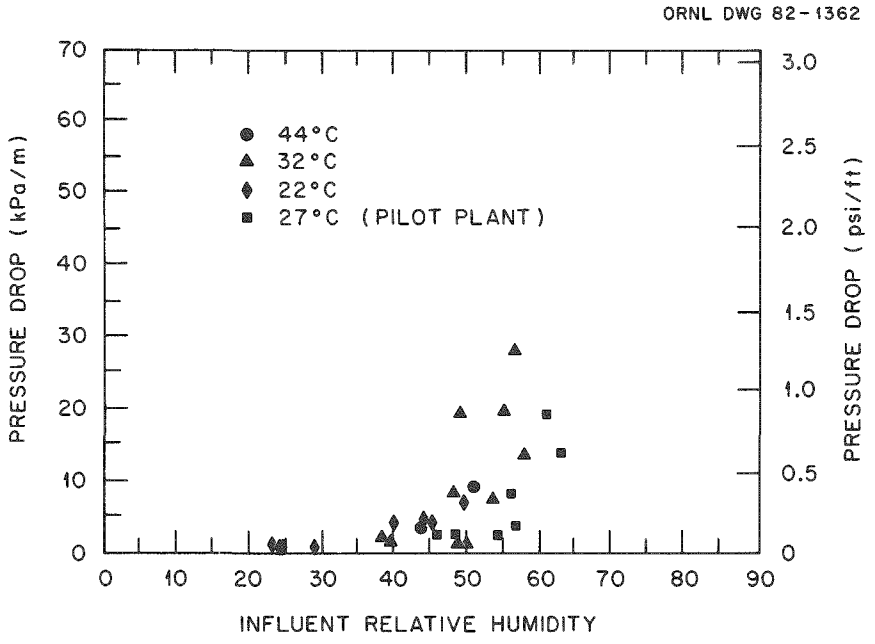

Fig. 11. Pressure drop as a function of influent relative humidity during isothermal and adiabatic fixed-bed studies on commercial $Ba(OH)_2 \cdot 8H_2O$ flakes (superficial gas velocity, ~13 cm/s).

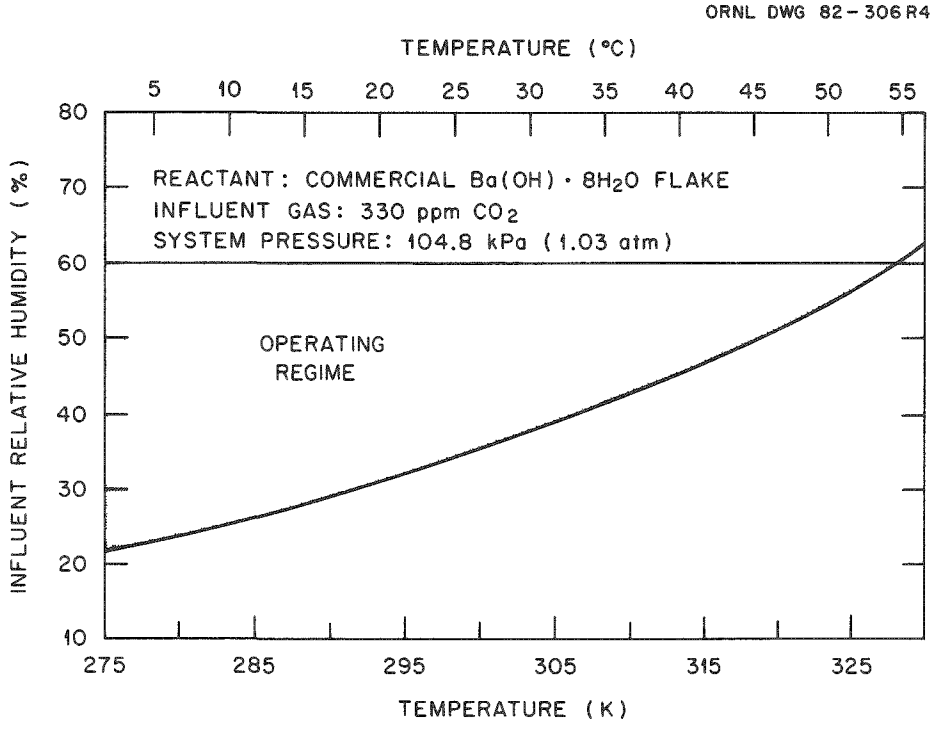

Fig. 12. Operating window for contacting a 330-ppmv-CO_2 gas stream with fixed beds of commercial $Ba(OH)_2 \cdot 8H_2O$ flakes (no prior conditioning or hydration step).

for $Ba(OH)_2 \cdot 8H_2O$ is valid, (2) the rate of dehydration or rehydration is proportional to the amount of free water on the surface (i.e., a function of relative humidity), and (3) the reactivity of $Ba(OH)_2 \cdot 8H_2O$ is 3 orders of magnitude greater than that of either $Ba(OH)_2 \cdot 3H_2O$ or $Ba(OH)_2 \cdot H_2O$. Macroscale studies under near-isothermal conditions on 10.2-cm-ID fixed beds of commercial $Ba(OH)_2 \cdot 8H_2O$ flakes and under near-adiabatic conditions on the pilot unit indicated that the pressure drop across the bed increased dramatically as 60% relative humidity in the influent gas was approached. It is speculated that this phenomenon results from the rapid rate of reaction at the entrance of the bed upon process start-up. The capillary condensation of water at V-shaped contact points or pores likely facilitates the rates of reaction, rehydration, and recrystallization of the flake at the higher relative humidities. Although the flakes hydrated at the high relative humidities have greater external surface area, they are more fragile and degrade more readily upon conversion to $BaCO_3$, thus also contributing to an increase in pressure drop.

Experimental studies indicated that the transfer of the reactant gas through the gas film is the major resistance to mass transfer. A model, assuming gas film control, was developed, and exact numerical solutions were obtained. An excellent correlation between the model-predicted breakthrough curves and the experimental breakthrough curves was obtained when the area available for mass transfer was modeled as a linear function of conversion [i.e., $A = A_0(1 - X)$]. The magnitude of the mass transfer coefficient was characteristic of literature values. There were indications that the magnitude of the initial surface area available for reaction, A_0, may be a weak function of velocity due to a realignment of the flakes. This realignment results from fluid shear forces and an accompanying reduction in the number of planar contact points between neighboring flakes, thus increasing the area available for mass transfer.

Based upon the experimental data obtained on beds under near-isothermal and near-adiabatic conditions, a window or regime of optimal process operation was determined to exist for the fixed-bed process. The window is bounded on the lower side by the dissociation vapor pressure of $Ba(OH)_2 \cdot 8H_2O$ and on the upper side by the onset of appreciable capillary

condensation and subsequent pressure drop problems (~60% relative humidity). An operating envelope is presented in Fig. 12 for the treatment of a 330-ppmv-CO_2 gas stream at a system pressure of 104.8 kPa (0.5 psig). The relative humidity of the influent gas must fall within the envelope for optimal gas throughput. If changes are made either in the CO_2 concentration, thus affecting the amount of water vapor produced, or in the system pressure, which will affect the partial pressure of the water vapor and subsequently the relative humidity (P/P_0), the operating envelope will change. The operating envelope also demonstrates why operational problems at 22 and 32°C were not severe and why considerable difficulty was encountered when attempting to operate the process at 42°C.

Based upon mechanistic arguments and the observed dependence upon influent relative huymidity, it was speculated that the pressure drop problem at relative humiditiese >60% may result from the more rapid rate of reaction at the reaction front during process start-up. If this should be the case, the pressure drop observed across downstream columns, which experience only pseudo-steady-state conversion and concentration profiles passing through them, should be reduced. Furthermore, the pressure drop problem should be reduced for more dilute CO_2-bearing gas streams (<330 ppm CO_2) and enhanced for gas streams that are richer in CO_2 due to corresponding localized rates of reaction upon process startup.

7. REFERENCES

1. H. Bonka et al., "Contamination of the Environment by Carbon-14 Produced in High-Temperature Reactors," *Kernetechnik* 15(7): 297 (1973).

2. W. Davis, Jr., *Carbon-14 Production in Nuclear Reactors*, ORNL/NUREG/TM-12 (1977).

3. C. O. Kunz, "Continuous Stack Sampling for ^{14}C at the R. E. Ginna Pressurized Water Reactor," *Trans. Am. Nucl. Soc.* 38: 100 (1981).

4. C. O. Kunz, W. E. Mahoney, and T. W. Miller, "Carbon-14 Gaseous Effluents from Boiling Water Reactors," *Trans. Am. Nucl. Soc.* 21: 91 (1975).

5. C. O. Kunz, W. E. Mahoney, and T. W. Miller, "C-14 Gaseous Effluent from Pressurized Water Reactors," pp. 229-34 in *Proceedings of the Health Physics Society 8th Midyear Symposium*, CONF-741018 (1974).

6. M. J. Kabat, "Monitoring and Removal of Gaseous Carbon-14 Species," in *Proceedings of the 15th DOE Nuclear Air Cleaning Conference*, CONF-780819 (1979).

7. H. Schuttelkopf, *Releases of $^{14}CO_2$ from Nuclear Facilities with Gaseous Effluents*, Kernsforschungszentrum Karlsruhe KFK 2421, June 1977 (translated from German) ORNL-tr-4527 (1978).

8. Exxon Nuclear Idaho Company, Inc., *Program Strategy Document for the Management of Radioactive Airborne Wastes — Draft*, prepared for Department of Energy, Idaho Operations Office (1981).

9. P. J. Magno, C. B. Nelson, and W. H. Ellett, "A Consideration of the Significance of Carbon-14 Discharges from the Nuclear Power Industry," p. 1047 in *Proceedings of the Thirteenth AEC Air Cleaning Conference*, CONF-740807 (1975).

10. G. G. Killough, "A Diffusion-Type Model of the Global Carbon Cycle for the Estimation of Dose to the World Population from Releases of Carbon-14 to the Atmosphere," ORNL/TM-5269 (1977).

11. G. G. Killough et al., *Progress Report on Evaluation of Potential Impact of ^{14}C Releases from an HTGR Reprocessing Facility*, ORNL/TM-5284 (1976).

12. L. Machta, "Prediction of CO_2 in the Atmosphere," in *Carbon and the Biosphere*, G. M. Goodwell and E. V. Pecan, Eds., Technical Information Center, Office of Information Services, U.S. Atomic Energy Commission (1973).

13. J. W. Snider and S. V. Kaye, "Process Behavior and Environmental Assessment of ^{14}C Releases from an HTGR Fuel Reprocessing Facility," in Proceedings of the ANS-AIChE Topical Meeting, Sun Valley, Idaho, Aug. 5-6, 1976.

14. L. Pauling, "Genetic and Somatic Effects of Carbon-14," *Science* 128: 1183 (1958).

15. J. Schwibach, H. Riedel, and J. Bretschneider, *Studies on the Emission of Carbon-14 from Nuclear Facilities (Nuclear Power Plants and Reprocessing Plants): Its Measurement and the Radiation Exposure Resulting from Emissions,* Series of the Institute for Radiation Hygiene of the Federal Health Office, No. 20 (translated from German), OLS-80-233, Oak Ridge National Laboratory (1979).

16. *Radiological Significance and Management of Tritium, Carbon-14, Krypton-85, Iodine-129 Arising from the Nuclear Fuel Cycle,* Nuclear Energy Agency, Organization for Economic Cooperation and Development, Paris, France (1980).

17. G. G. Killough and P. S. Rohwer, "A New Look at the Dosimetry of ^{14}C Released to the Atomsphere as Carbon Dioxide," *Health Phys.* 4: 141 (1978).

18. G. G. Killough et al., "Dose Equivalent due to Atmospheric Releases of Carbon, Chap. 11 in *Models and Parameters for Environmental Radiological Assessment,* C. W. Miller, Ed., DOE/TIC-11368 (in press).

19. G. G. Killough and J. E. Till, "Scenarios of ^{14}C Releases from the World Nuclear Industry from 1975 to 2020 and the Estimated Radiological Impact," *Nucl. Saf.* 19(5): 602 (1978).

20. T. W. Fowler and C. B. Nelson, *Health Impact Assessment of Carbon-14 Emissions from Normal Operations of Uranium Fuel Cycle Facilities,* EPA 520/5-80-004 (1981).

21. G. L. Haag, "Carbon-14 Immobilization via the CO_2—$Ba(OH)_2$ Hydrate Gas-Solid Reaction, in *Proceedings of the 16th DOE Nuclear Air Cleaning Conference,* CONF-801038 (1981).

22. *Handbook of Chemistry and Physics,* 52nd ed., The Chemical Rubber Co., Cleveland, Ohio, 1972, pp. 13-70.

23. W. F. Linke and A. Seidell, *Solubilities of Inorganic and Metal Organic Compounds,* 4th ed., American Chemical Society, Washington, D.C., 1958.

24. A. G. Croff, *An Evaluation of Options Relative to the Fixation and Disposal of ^{14}C-Contaminated CO_2 as $CaCO_3$,* ORNL/TM-5171 (1976).

25. A. G. Evans et al., *Management of Radioactive Waste Gases from the Nuclear Fuel Cycle — Volume 1, Comparison of Alternatives,* NUREG/CR-1546, DPST-NUREG-80-5, vol. 1 (1980).

26. D. W. Holladay, *Experiments with a Lime Slurry in a Stirred Tank for the Fixation of Carbon-14 Contaminated CO_2 from Simulated HTGR Fuel Reprocessing Off-Gas,* ORNL/TM-5757 (1978).

27. D. W. Holladay, *An Experimental Investigation of the Distribution of Krypton from Simulated HTGR Fuel Reprocessing Off-Gas During the Removal and Fixation of CO_2 by the CO_2-$Ca(OH)_2$ Slurry Reaction,* ORNL/TM-6539, (1982).

28. D. W. Holladay and G. L. Haag, "Removal of ^{14}C-Contaminated CO_2 from Simulated LWR Fuel Reprocessing Off-Gas by Utilizing the Reaction Between CO_2 and Alkaline Hydroxides in Either Slurry or Solid Form," pp. 548-69 in *Proceedings of the 15th DOE Nuclear Air Cleaning Conference,* CONF-780819 (1979).

29. K. J. Notz et al., "Processes for the Control of $^{14}CO_2$ During Reprocessing," presented at the International Symposium on Management of Gaseous Wastes from Nuclear Facilities, Vienna, Austria, Feb. 18-22, 1980.

30. G. R. Bray et al., *Assessment of Carbon-14 Control Technology and Costs for the LWR Fuel Cycle,* EPA 520/4-77-013 (1977).

31. J. L. Kovach, *Review of Carbon-14 Control Technology and Cost,* NUCON 8EP555/01, Nuclear Consulting Services, Inc., Columbus, Ohio (1979).

32. G. L. Haag, *Application of the CO_2-$Ba(OH)_2 \cdot 8H_2O$ Gas-Solid Reaction for the Treatment of Dilute CO_2-Bearing Gas Streams,* Ph.D. Dissertation, University of Tennessee, Knoxville, 1982; to be published as ORNL-5887.

33. G. L. Haag, G. C. Young, and J. W. Nehls, Jr., "Pilot Unit Development of the CO_2-$Ba(OH)_2 \cdot 8H_2O$ Gas-Solid Reaction for ^{14}C Immobilization," to be published as ORNL/TM-8433.

34. J. Nillis, Sherwin Williams Co., Coffeeville, Kans., personal communication to G. L. Haag, 1981.

35. M. Michaud, "Contribution to the Study of the Hydroxides of Potassium and Barium," *Rev. Chim. Minerale* t.5: 89 (1968).

36. M. Michaud, "Inorganic Chemistry — Study of the Binary Water—Barium Hydroxide System," C. R. Acad. Sci. Paris 262.CV: 1143 (1966).

37. B. A. Kondakov, P. V. Kovtunenko, and A. A. Bundel, "Equilibria Between Gaseous and Condensed Phases in the Barium Oxide—Water System.," *Russ. J. Phys. Chem.* 38(1): 99-102 (1964).

ORNL-5926
Dist. Category UC-70

INTERNAL DISTRIBUTION

1. S. I. Auerbach
2. J. O. Blomeke
3. W. D. Bond
4. W. D. Burch
5. C. H. Byers
6. D. O. Campbell
7. J. L. Collins
8. J. H. Coobs
9. R. M. Counce
10. A. G. Croff
11. L. R. Dole
12. R. S. Eby
13. C. S. Fore
14. H. W. Godbee
15-19. G. L. Haag
20. D. C. Hampson
21. A. L. Harkey
22. R. T. Jubin
23. P. R. Kasten
24. M. V. Keigan
25. J. H. Kessler
26. L. J. King
27. E. H. Krieg, Jr.
28. W. J. Lackey
29. R. E. Leuze
30. D. K. Little
31. A. P. Malinauskas
32. E. W. McDaniel
33-37. J. W. Nehls, Jr.
38. K. J. Notz
39. F. L. Peishel
40. W. W. Pitt, Jr.
41. D. J. Pruett
42. T. H. Row
43. M. B. Sears
44. M. G. Stewart
45. J. R. Stokely
46. S. M. Tiegs
47. J. E. Vath
48. J. S. Watson
49. S. K. Whatley
50. J. E. Wortman
51-55. G. C. Young
56-57. Central Research Library
58. ORNL—Y-12 Technical Library
Document Reference Section
59-60. Laboratory Records Department
61. Laboratory Records, ORNL RC
62. ORNL Patent Section

EXTERNAL DISTRIBUTION

63. A. L. Ayers, EG&G Idaho, Inc., P.O. Box 1625, Idaho Falls, ID 83401
64. R. H. Beers, Idaho Operations Office, Department of Energy, 550 Second Street, Idaho Falls, ID 83401
65. W. F. Bennett, Rocky Flats Area Office, P.O. Box 928, Golden, CO 80401
66. W. Bergman, Lawrence Livermore Laboratory, P.O. Box 808, Livermore, CA 94550
67. L. C. Borduin, Los Alamos Scientific Laboratory, P.O. Box 1663, Los Alamos NM 87544
68. R. A. Brown, Exxon Nuclear Idaho Company, Inc., P.O. Box 2800, Idaho Falls, ID 83401
69. L. L. Burger, Battelle Pacific Northwest Laboratory, P.O. Box 999, Richland, WA 99352
70. R. H. Campbell, Manager, Uranium Mine Tailings Remedial Program, U.S. Department of Energy, Albuquerque Operations Office, Actions Office, P.O. Box 5400, Albuquerque, NM 87115

71. W. A. Carbiener, Office of Nuclear Waste Isolation, Battelle Project Office, 505 King Avenue, Columbus, OH 43201
72. K. A. Carlson, Idaho Operations Office, U.S. Department of Energy, 550 Second Street, Idaho Falls, ID 83401
73. T. D. Chikalla, Battelle-Pacific Northwest Laboratory, P.O. Box 999, Richland, WA 99352
74. J. D. Christian, Exxon Nuclear Idaho Co., Inc., P.O. Box 2800, Idaho Falls, ID 83401
75. J. L. Crandall, Director, Savannah River Laboratory, P.O. Box A, Aiken, SC 29801
76. G. H. Daly, Technology Division, Office of Waste Operations and Technology, U.S. Department of Energy, Mail Stop B-107, Washington, DC 20545
77. R. Danford, Attn: Input Processing Division, Institute for Research and Evaluation, 21098 IRE Control Center, Eagen, MN 55121
78. M. M. Dare, Oak Ridge Operations, U.S. Department of Energy, P.O. Box E, Oak Ridge, TN 37830
79. J. E. Dieckhoner, Operations Division, Office of Waste Operations and Technology, U.S. Department of Energy, Mail Stop B-107, Washington, DC 20545
80. P. T. Dickman, EG&G Idaho, Inc., P. O. Box 1625, Idaho Falls, ID 83401
81. M. W. First, Harvard Air Cleaning Laboratory, 665 Huntington Ave., Boston, MA 02115
82. R. G. Garvin, Savannah River Laboratory, P.O. Box A, Aiken, SC 29801
83. W. S. Gregory, Los Alamos Scientific Laboratory, P.O. Box 1663, Los Alamos, NM 87544
84. J. P. Hamric, Idaho Operations Office, U.S. Department of Energy, 550 Second Street, Idaho Falls, ID 83401
85. E. C. Hardin, Albuquerque Operations Office, U.S. Department of Energy, P.O. Box 5400, Albuquerque, NM 87115
86. C. A. Heath, Office of Waste Isolation, U.S. Department of Energy, Mail Stop B-107, Washington, DC 20545
87. L. L. Hench, Division of Materials Science and Engineering, University of Florida, Gainesville, FL 32611
88. E. L. Keller, Oak Ridge Operations, U.S. Department of Energy, P.O. Box E, Oak Ridge, TN 37830
89. R. G. Kepler, Organic and Electronic, Department 5810, Sandia Laboratories, Albuquerque, NM 87185
90. J. H. Kittel, Office of Waste Management Programs, Argonne National Laboratory, 9700 South Cass Avenue, Argonne, IL 60439
91. D. A. Knecht, Exxon Nuclear Idaho, Inc., P. O. Box 2800, Idaho Falls, ID 83401
92. T. Kyle, Los Alamos Scientific Laboratory, P. O. Box 1663, Los Alamos, NM 87544
93. J. L. Landers, Division of Waste Products, Mail Stop B-107, U.S. Department of Energy, Germantown, MD 20545
94. J. R. Landon, Richland Operations Office, U.S. Department of Energy, P.O. Box 550, Richland, WA 99352
95. L. Lani, Nuclear and Magnetic Fusion Division, San Francisco Operations Office, U.S. Department of Energy, 1333 Broadway, Oakland, CA 94612

96. D. E. Large, Manager, ORO Radioactive Waste Management Programs, U.S. Department of Energy, Oak Ridge Operations, Oak Ridge, TN 37830
97. M. J. Lawrence, Acting Director, Office of the Director, Office of Transportation and Fuel Storage, NE-340 Mail Stop B-107, U.S. Department of Energy, Germantown, MD 20545
98. M. Lencoe, Office of Nuclear Waste Isolation, Battelle Project Office, 505 King Avenue, Columbus, OH 43201
99. R. Y. Lowrey, Chief, Waste Management Branch, Weapons Production Division, U.S. Department of Energy, Albuquerque Operations Office, P.O. Box 5400, Albuquerque, NM 87115
100. R. Maher, Waste Management Programs, Savannah River Plant, E. I. du Pont de Nemours and Company, Aiken, SC 29801
101. S. A. Mann, Chicago Operations and Regional Office, U.S Department of Energy, Argonne, IL 60439
102. A. B. Martin, Rockwell International, Energy Systems Group, 8900 DeSoto Avenue, Canoga Park, CA 91304
103. E. F. Mastel, Planning and Analysis Division, Office of Resource Management and Planning, Mail Stop B-107, U.S. Department of Energy, Germantown, MD 20545
104. M. D. McCormack, EG&G Idaho, Inc., P.O. Box 1625, Idaho Falls, ID 83401
105. J. R. McDonald, Naval Research Laboratory, Code 6110, Washington, DC 20375
106. D. J. McGoff, Projects Division, Office of Waste Operations and Technlogy, U.S. Department of Energy, Mail Stop B-107, Washington, DC 20545
107. R. J. Merlini, Rockwell International, Atomics International Division, Rocky Flats Plant, P.O. Box 464, Golden, CO 80401
108. S. Meyers/R. Romatowski, Office of Nuclear Waste Management, U.S. Department of Energy, Mail Stop B-107, Washington DC 20545
109. B. G. Motes, Exxon Nuclear Idaho, Inc., P.O. Box 2800, Idaho Falls, ID 83401
110. J. O. Neff, Program Manager, NWTS Program Office, U.S. Department of Energy, 505 King Avenue, Columbus, OH 43201
111. G. K. Oertel, Director, Office of Waste Operations and Technology, Mail Stop B-107, U.S. Department of Energy Germantown, MD 20545
112. H. Palmour III, 2140 Burlington Engineering Laboratories, North Carolina State University, Raleigh, NC 27607
113. R. W. Passmore, EG&G Idaho, Inc., P. O. Box 1625, Idaho Falls, ID 83401
114. J. W. Peel, Idaho Operations Office, Department of Energy, 550 Second Street, Idaho Falls, ID 83401
115. R. W. Ramsey, Acting Program Manager, Remedial Action Program, Division of Waste Products, Mail Stop B-107 (NE-30), U.S. Department of Energy, Germantown, MD 20545
116. M. L. Rogers, Monsanto Research Corporation, Mound Facility, P.O. Box 32, Miamisburg, OH 45342
117. Rustum Roy, 202 Materials Research Laboratory, Pennsylvania State University, University Park, PA 16802

118. J. J. Schriber, Manager, Waste Management Division, Richland Operations Office, U.S. Department of Energy, Richland, WA 99352
119. M. J. Steindler, Chemical Engineering Division, Argonne National Laboratory, 9700 Cass Avenue, Argonne, IL 60439
120. A. L. Taboas, TRU Program Manager, Waste Management Branch, U.S. Department of Energy, Albuquerque, NM 87115
121. T. R. Thomas, Exxon Nuclear Idaho Co., Inc., P.O. Box 2800, Idaho Falls, ID 83401
122. Major Thompson, E. I. du Pont de Nemours, Savannah River Laboratory, Aiken, SC 29801
123. G. T. Tingey, Battelle Pacific Northwest Laboratory, P.O. Box 999, Richland, WA 99352
124. R. D. Walton, Technology Division, Office of Waste Operations and Technology, U.S. Department of Energy, Mail Stop B-107, Washington, DC 20545
125. R. P. Whitfield, Savannah River Operations, Aiken, SC 29801
126. J. B. Whitsett, Radioactive Waste Programs Branch, Nuclear Fuel Cycle Division, Idaho Operations Office, 550 Second Street, Idaho Falls, ID 83401
127. B. Wilson, Savannah River Operations Office, U.S. Department of Energy, P.O. Box A, Aiken, SC 29801
128. C. B. Bartlett, Chief, Fuel Cycle Research Branch, Division of Fuel Cycle and Environmental Research, U.S. Nuclear Regulatory Commission, Mail Stop SS-1130, Washington, DC 20555
129. S. J. Beard, Fuel Reprocessing Engineering, Exxon Nuclear Company, Inc., 777 106th Avenue, NE, Bellevue, WA 98009
130. J. A. Buckham, Allied-General Nuclear Services, P.O. Box 847, Barnwell, SC 29812
131. J. P. Duckworth, Nuclear Fuel Services, Inc., P.O. Box 124, West Valley, NY 14174
132. B. F. Judson, General Electric Company, 175 Curtner Avenue, M/C 858, San Jose, CA 95125
133. W. H. Lewis, Vice President, Nuclear Fuel Services, Inc., 6000 Executive Blvd., Rockville, MD 20852
134. Hayne Palmour III, 2140 Burlington Engineering Laboratories, North Carolina State University, Raleigh, NC 27607
135. R. E. Tomlinson, Manager, Exxon Nuclear Co., Inc., 2101 Horen Rapids Road, Richland, WA 99352
136. Dr. Ken Brog, Battelle-Columbus Laboratories, 505 King Avenue, Columbus, OH 43201
137. D. L. Ulrichson, Iowa State University, Ames, IA 50010
138. P. H. Emmet, Portland State University, Portland, OR
139. A. Kitana, Tokyo Electric Power Company, Inc., 1901 L Street, Northwest, Suite 720, Washington, DC 20036
140. V. Trevorrow, Argonne National Laboratory, 9700 South Cass Avenue, Argonne, IL 60439
141. S. Strausberg, General Atomic Corp., P.O. Box 81608, San Diego, CA 92138
142. J. Nillis, Sherwin Williams Company, Coffeeville, KS
143. M. H. Lietzke, Chemistry Department, The University of Tennessee, Knoxville, TN 37916

144. D. Pence, Science Applications, 4030 Sorrento Valley Boulevard, San Diego, CA 92124
145. M. First, Harvard School of Public Health, 65 Huntington Avenue, Boston, AM 02115
146. C. H. Cheh, Ontario Hydro Research Division, 800 Kipling Avenue, Toronto, Ontario, M8Z5S4, Canada
147. V. R. Deitz, Naval Research Laboratory, Code 6170, Washington, DC
148. A. G. Evans, E. I. du Pont de Nemours, Savannah River Laboratory, Aiken, SC
149. M. Kabat, Ontario Hydro, Toronto, Canada
150. J. L. Kovach, Nuclear Consulting Services, Inc., P.O. Box 29151, Columbus, OH 43229
151. Charles Kunz, N.Y. State Department of Health, Albany, NY
152. Paul Monson, E. I. du Pont de Nemours, Savannah River Laboratory, Aiken, SC 29808
153. A. C. Vikis, Atomic Energy of Canada Ltd., Pinawa, Manitoba, Canada, ROE 1LO
154. Margaret A. Widmayer, U.S. Department of Energy, 550 Second Street, Idaho Falls, ID 83401
155. Ed Clark, Department of Chemical Engineering, University of Tennessee, Knoxville, TN 37916
156. George Frazier, Department of Chemical Engineering, University of Tennessee, Knoxville, TN 37916
157. R. Nelson, AERE Harwell, England
158. G. Fraser, Commission of the European Communities (DG V/E/2) Batiment Jean Monnet (C 4/123), Palteau de Kirchberg, G. D. de Luxembourg
159. G. Schwaarz, Luisenstrasse 37, D-5100, AACHEN, Federal Republic of Germany
160. E. Henrich, Kernforschungszentrum Karlsruhe (KFK), Institute of Hot Chemistry, 7500 Karsruhe, Postfach 3640, Federal Republic of Germany
161. R. Jokoll, Sektion Chemie der Friedrich-Schiller-Univeresitat, DDR — 69 Jena, Steiger 3, Haus III
162. H.-P. Wichmann, GWK., Bruschsal 3, Hauptmann 21b, Federal Republic of Germany, 7520.
163. J. Wilhelm, KFK, Karlsruhe, Postfach 3640, D-7000, Federal Republic of Germany
164. R.-D. Penzhorn, KFK, Karlsruhe, Postfach 3640, D-7500, Federal Republic of Germany
165. F. J. Herrmann, GWK, Karlsruhe, 7514 Eggentsein, Hayon Str 10A, Federal Republic of Germany 7514
166. E. Henrich, KFK, Karlsruhe, Postfach 3640, D-7500, Federal Republic of Germany
167. J. Furrer, KFK, Karlsruhe, Postfach 3640, D-7500, Federal Republic of Germany
168. H. Ringel, Kernforschungsanlage Julich, Federal Republic of Germany
169. R. Von Ammon, Kernforschungazetrum, Karlsruhe, Federal Republic of Germany
170. J. G. Wilhelm, Nuclear Reserach Center, Karlsruhe, Federal Republic of Germany
171. L. Trevorrow, Argonne National Laboratory, CMT-205, 9700 S. Cass Avenue, Argonne, IL 60439

172. Office of Assistant Manager for Energy Research and Development, DOE-ORO, P.O. Box E, Oak Ridge, TN 37830

173-485. Given distribution as shown in TID-4500 under Nuclear Waste Management Category, UC-70.

☆ U S GOVERNMENT PRINTING OFFICE 1983 646 055 315